



# Structural characterization of a special boundary between $\alpha$ plates after martensitic transformation in cobalt



Jian Tu <sup>\*</sup>, Songquan Zhang, Zhiming Zhou, Hailong Tang

School of Materials Science and Engineering, Chongqing University of Technology, Chongqing 400054, China

## ARTICLE INFO

### Article history:

Received 1 September 2015  
Received in revised form 20 December 2015  
Accepted 22 December 2015  
Available online 30 December 2015

### Keywords:

Phase boundary  
Martensitic transformation  
Cobalt

## ABSTRACT

In this study, the interfacial structure of a special boundary between  $\alpha$  plates in cobalt after martensitic transformation was characterized and investigated in detail, by using transmission electron microscopy (TEM) and high-resolution TEM. It was found that the boundaries with the special misorientation  $(71.4^\circ / \langle 11\bar{2}0 \rangle)$  consist of  $(0001) // (10\bar{1}1)$  basal–pyramidal interfaces and steps. This special misorientation relationship  $(71.4^\circ / \langle 11\bar{2}0 \rangle)$  between  $\alpha$  plates should be identified as one common misorientation relationship.

© 2015 Published by Elsevier Inc.

## 1. Introduction

Cobalt (Co) and Co-based alloys have been widely used in many magnetic applications [1–3]. Co undergo an allotropic transformation between two close-packed structures, hexagonal closed-packed ( $\alpha$  phase) and face center cubic ( $\beta$  phase) [4–6]. This transformation exhibits a characteristic of martensitic transformation. It is worth noting that  $\beta$  phase can't completely transform into  $\alpha$  phase in Co after martensitic transformation [7–9], so a mixture of hexagonal closed-packed (HCP) and face center cubic (FCC) phases in Co will cause the poor magnetic properties [10,11]. Thus, it would be crucial to understand the martensitic transformation in Co for its application as magnetic recording media.

Interestingly, a high fraction of special misorientation  $(71.4^\circ / \langle 11\bar{2}0 \rangle)$  was observed between  $\alpha$  plates in Co [12]. This special misorientation was correlated to the transformation twins (the twinning relationship). However, it has long been recognized that  $\alpha$  and  $\beta$  phases in Co can be related by the orientation relationship [4]:  $\{111\}_\alpha // \{0001\}_\beta$  and  $\langle 110 \rangle_\alpha // \langle 11\bar{2}0 \rangle_\beta$ . Thus,  $71.4^\circ / \langle 11\bar{2}0 \rangle$  misorientation can be deduced as the common misorientation relationship [13]. Because the common misorientation relationship is distinctly different from the twinning relationship, the essence of such a special boundary  $(71.4^\circ / \langle 11\bar{2}0 \rangle)$  between  $\alpha$  plates should be investigated.

To address the controversial question, in the present work, this special boundary  $(71.4^\circ / \langle 11\bar{2}0 \rangle)$  was characterized by means of scanning electron microscope (SEM), SEM-Electron Back-Scattered Diffraction

(SEM-EBSD), transmission electron microscopy (TEM) and high-resolution TEM (HRTEM), and further investigated in detail with the expectation to yield definite answers in this work.

## 2. Experimental

Polycrystalline Co (99.9% purity) sheets used in this work were acquired from Goodfellow Company. The deformed specimens (strain up to 8%) were sealed into a quartz tube under the vacuum condition. The specimens were annealed in a Lenton PTF 1200 °C-Tube furnace at 973 K for 48 h, and these specimens were cooled to room temperature in the furnace. The pre-deformation aimed at introducing more defects to yield smaller recrystallized grains after annealing. Subsequently, the heat-treated specimens were analyzed by SEM, SEM-EBSD, TEM and HRTEM measurements. The microstructures of specimens were characterized by electron channeling contrast (ECC) and secondary electron (SE) imaging techniques in a Zeiss Sigma HD field emission gun scanning electron microscope (FEG-SEM). In order to achieve the surface quality required for EBSD examination, electropolishing was conducted at 20 V/0.5A at room temperature for 50 s in a solution, which consisted of 10 ml glycerin, 20 ml perchloric acid and 71 ml alcohol. The EBSD patterns were processed by using the Channel 5 software from HKL technology to determine the local misorientations. For TEM measurement, the samples with 0.4 mm thickness were sectioned by spark-cutting and thinned by grinding, and then electropolished through twin-jet polisher in a solution of 10% perchloric acid and 90% glacial acetic acid at a voltage of 50 V at room temperature. TEM measurements were carried out with on FEI Tecnai F30-G<sup>2</sup> electron microscope at an operating at voltage of 300 kV.

<sup>\*</sup> Corresponding author.  
E-mail address: [tujian@cqut.edu.cn](mailto:tujian@cqut.edu.cn) (J. Tu).

### 3. Results and discussion

Fig. 1 shows the microstructures of  $\alpha$  plates in Co after phase transformation. As shown in Fig. 1a,  $\alpha$  plates exhibit different contrast in ECC images, suggesting these  $\alpha$  plates may belong to the different  $\alpha$  variants with the different crystallographic orientations. Furthermore, surface relief is clearly revealed in SE image, as shown in Fig. 1b. The surface relief in  $\alpha$  plates exhibits the triangular and rectangle morphology. It is also evident that the areas between the surface relief lines remain unaffected by phase transformation, suggesting that the phase transformation in Co was localized and incomplete.

To perform quantitative analyses on the orientation relationship between  $\alpha$  plates, an EBSD scan was conducted. After a standard noise reduction procedure, the complete EBSD map is shown in Fig. 2a, which is reconstructed from the special boundary superposed by band contrast map. A global misorientation measurement is revealed in Fig. 2b, and a remarkable peak around  $71.4^\circ$  can be seen from the misorientation angle distribution histogram. The analysis on rotation axes of misorientation angles around  $71.4^\circ$  reveals the axes are close to  $\langle 11\bar{2}0 \rangle$  (red arrow in Fig. 2b). Therefore, the special boundaries (marked by red lines in Fig. 2a) with special misorientation ( $71.4^\circ / \langle 11\bar{2}0 \rangle$ ) can be observed in this work.

In consideration of the limitations of EBSD technology, TEM and HRTEM were employed to characterize the special boundary. Fig. 3a exhibits the morphology of the boundaries with the special misorientation between HCP<sub>1</sub> and HCP<sub>2</sub> is straight by TEM. The corresponding selected-area electron diffraction (SAED) patterns taken using the  $[1\bar{2}10]$  zone axis are indicated by the red circle across the boundary (Fig. 3a). The misorientation between HCP<sub>1</sub> and HCP<sub>2</sub> is  $71^\circ$ , as shown in Fig. 3b.

The boundaries between HCP<sub>1</sub> and HCP<sub>2</sub> (marked by yellow dotted frames, Area 1 in Fig. 3a) were further investigated by HRTEM, as shown in Fig. 3c. One typical microstructure feature, the abundant basal stacking faults (SFs) in HCP<sub>1</sub> and HCP<sub>2</sub> phases, can be observed. SFs play an important role in FCC  $\rightarrow$  HCP martensitic transformation [4]. The expansion and shrinkage of SFs via the movement of the  $\frac{2}{3}\langle 112 \rangle$  Shockley partial dislocations along  $\{111\}$  planes in FCC structure lead to FCC  $\rightarrow$  HCP transformation [4], so a coordinated activation of  $\frac{2}{3}\langle 112 \rangle$  gliding on every second  $\{111\}$  plane is required. If SFs are introduced on every second  $\{111\}$  atomic plane of FCC structure, the stacking sequence on the plane will change from the FCC structure (...ABCABCABC...) to the HCP structure (...ABABAB...). However, there may be no unequivocal mechanisms for the “filling in” between faults to create a perfect HCP structure, so SFs can be left accompanying with the phase transformation [14–17].

In Fig. 3c, the (0002) basal planes (marked by red dotted line) aren't reflected about the boundary between HCP<sub>1</sub> and HCP<sub>2</sub>, indicating that this special boundary may not be the twinning boundary. Area 2 (marked by yellow dotted frames in Fig. 3c) at a higher magnification

is shown in Fig. 3d. The boundary seems to be straight, not too coarse. To examine the structural characteristics of this special boundary, the area 3 and area 4 (marked by yellow dotted frames) are amplified, as shown in Fig. 4. Fourier filtration was applied to produce filtered HRTEM images of the area 3 and area 4 (Fig. 3d), as shown in Fig. 4a and b, respectively. As we can see, the actual boundary presents a faceted structure (incoherent), and this special boundary consists of a series of steps (yellow broken lines denoted by green arrows) joining with straight terraces (red lines denoted by yellow arrows).

The structural characterizations of the special boundary in Fig. 4 are analyzed as follows. Firstly, these steps referred to defects play a central role in diffusionless transformation for phase transformation. Two excellent reviews related to the mobility of interfacial defects in martensitic transformations are shown in Ref. [18,19], suggesting that the diffusive flux of material is associated with the motion of line defects along an interface. Secondly, the straight terraces are consistent with (0001)//(10 $\bar{1}$ 1) basal–pyramidal (BPy) orientation, which places basal planes and pyramidal planes face to face in HCP lattices. Interestingly, the (0001)//(10 $\bar{1}$ 1) BPy interface is also observed in  $\{10\bar{1}3\}$  twin by HRTEM, while this interface is responsible for the deviation of the actual  $\{10\bar{1}3\}$  TB from the theoretical twinning plane ( $K_1$  plane) [20]. In connection with the structural characterizations of the special boundary, two important issues should be addressed: (i) for such special boundary, is it a twinning relationship or a common misorientation relationship? (ii) What is the formation mechanism for such special boundary?

This boundary with special misorientation relationship ( $71.4^\circ / \langle 11\bar{2}0 \rangle$ ) exhibits straight morphology, which are typically observed for the annealing twin boundaries. Thus, some authors suggested such special boundary is a twinning boundary [12]. However, this evidence is obviously inadequate. The present authors have two solid evidences to prove that the special orientation relationship ( $71.4^\circ / \langle 11\bar{2}0 \rangle$ ) between  $\alpha$  plates is the common misorientation relationship. Firstly, we review the definition of the twin [21]: a “twin” which is the crystal structure is identical with the “parent”, but orientated differently. Because the two structures are identical, the interface must remain invariant during twinning (twinning plane). Therefore, the parent and the twin lattices should be reflected about the twinning plane. However, the (0002) basal planes in HCP<sub>1</sub> and HCP<sub>2</sub> are not mirrored by this special boundary, as shown in Figs. 3 and 4. Thus, this special boundary without the special symmetry is not the twinning boundary. Secondly, the SAED pattern (Fig. 3b) suggests that two sets of diffraction spots don't show the common spot, so the misorientation between the two neighboring crystals can't be considered as the twinning relationship. Thus, we can confirm that the twinning relationship between  $\alpha$  plates with special misorientation ( $71.4^\circ / \langle 11\bar{2}0 \rangle$ ) in Co is incorrect, and the misunderstanding on this orientation features of  $\alpha$ -plate boundaries is clarified. It is worth noting that the same conclusion is also revealed in Zr

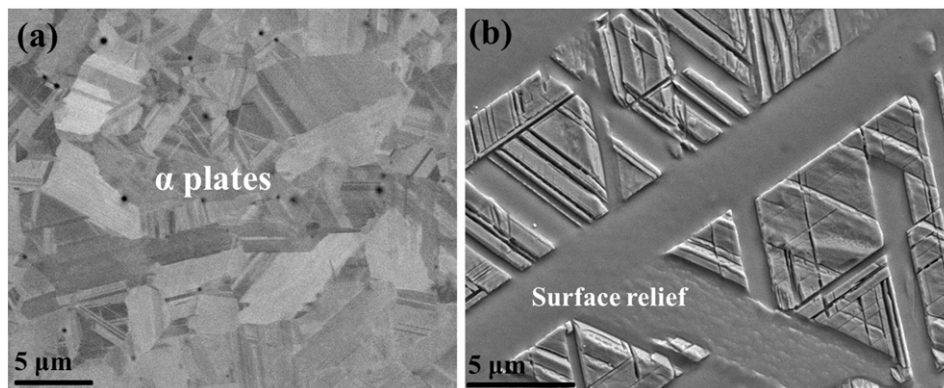


Fig. 1. (a) ECC image showing microstructure of Co after martensitic transformation; (b) SE image showing surface relief between plates.

Download English Version:

<https://daneshyari.com/en/article/1570618>

Download Persian Version:

<https://daneshyari.com/article/1570618>

[Daneshyari.com](https://daneshyari.com)